



# A novel compressive sampling method for ECG wearable measurement systems

Francesco Picariello, Grazia Iadarola, Eulalia Balestrieri, Ioan Tudosa, Luca De Vito\*

Department of Engineering, University of Sannio, Piazza Roma, 21, 82100 Benevento, Italy

## ARTICLE INFO

### Article history:

Received 18 May 2020

Received in revised form 29 June 2020

Accepted 15 July 2020

Available online 26 July 2020

### Keywords:

Internet-of-Medical-Things

Wearable measurement systems

ECG signal

Compressive sampling

Sampling method

## ABSTRACT

The paper presents a novel method for the compressed acquisition of electrocardiographic (ECG) signals. The proposed method is intended to be applied to Internet-of-Medical-Things (IoMT) acquisition nodes (i.e. wearable measurement systems) as they can benefit from a reduction of the signal data rate to be transmitted, and the consequent reduction of energy consumption. Being based on Compressive Sampling (CS), the proposed method presents a very low computational complexity on the acquisition node. Moreover, since the sensing matrix is adapted to the acquired signal, it allows achieving a better reconstruction performance compared with the other CS-based methods available in literature.

© 2020 Published by Elsevier Ltd.

## 1. Introduction

In recent years, wearable measurement systems for measuring physiological signals and parameters are becoming more complex due to the integration of several sensors and electronic front-ends, allowing to observe and real-time transmit signals, such as electrocardiogram (ECG) and respiration wave. Moreover, they are going to be integrated in Internet-of-Things (IoT) systems where several acquisition nodes must be connected and managed. In particular, in this field, Internet-of-Medical-Things (IoMT) systems have been proposed to monitor and manage healthcare applications [1,2].

One of the main challenges of IoMT nodes is to meet the energy consumption and size requirements of wearable devices. Moreover, IoMT systems must collect and store data from up to thousands of nodes, resulting in a significant data rate to be handled. A possible compression of this data rate must however guarantee a biosignal integrity, able to comply with medical standards, when it is necessary. Such challenges becomes harder as IoMT nodes are going to include not only Personal Area Network (PAN), but also Wireless Wide Area Network interfaces, such as Wi-Fi, LoRa, Sigfox or Narrowband-IoT (NB-IoT), which are characterized by higher power consumptions and lower data rates.

Compression of biosignals has been proposed as a way both to reduce the data rate that the IoMT node has to transmit and to reduce the energy consumption of the node [3], since in many

cases data transmission is the most expensive activity in terms of energy. In particular, among the different biosignals, the compression of the ECG has been faced by many researchers. A first classification of research contributions regarding ECG compression can be made by distinguish hardware and hybrid methods from digital methods. Methods in the former category exploit the sparsity of ECG signal in the time domain to design optimized architectures of analog-to-digital conversion. A method falling in this category is proposed in [4], where the authors designed a level-crossing Analog-to-Digital Converter (ADC) to efficiently sample analog ECG signals. The advantage of solutions in this category is that they provide signal compression without any computational load for the microcontroller of the acquisition node. Beside that, they rely on specific hardware designs that must be integrated in the acquisition node. For this last reason, in most cases a complete digital solution is preferred. The papers falling in the category of digital methods can be further classified into three types: direct methods, parameter extraction methods and transform domain methods [5]. Direct methods achieve compression by removing the redundancy of the ECG signal in the time domain. A method belonging to this type, described in [6], proposed a protocol for ECG data compression where ECG data are coded as ASCII characters.

In [7], the authors proposed a dynamic compression scheme for ultra-low power and real-time wireless ECG applications. It consisted of a digital integrate-and-fire sampler, allowing to represent the ECG signal as a pulse train and a lossless entropy encoder, allowing to encode the timestamps and sign phases of the pulse train to a binary stream. Parameter extraction methods are based

\* Corresponding author.

E-mail address: [devito@unisannio.it](mailto:devito@unisannio.it) (L. De Vito).

on the extraction of some features of the ECG signal such as the P wave (the earliest wave of the ECG cycle, corresponding to the atria depolarization), the T wave (corresponding to the repolarization of the ventricles) or the QRS complex (corresponding to the depolarization of the right and left ventricles). A method falling in this category was presented in [8]. This method is composed by a preprocessing phase, where the signal is divided in beats and each beat is further segmented to find the P section, the QRS section and the T section. Each section is filtered with a different filter and the baseline is removed. Then, an encoder searches the best match of the preprocessed beat with the entries of a codebook and performs a Long-Term Prediction (LTP). Finally, the residue between the output of the codebook and the predicted waveform from the LTP is furtherly coded. In transform domain methods, the ECG signal is projected to a transform domain by means of a linear orthogonal transformation. Then the coefficients in the transformed domain are properly encoded. Some widely used transforms include Discrete Fourier Transform (DFT), Discrete Cosine Transform (DCT), Walsh Transform and Discrete Wavelet Transform (DWT) [5,9]. In [10], the ECG is compressed by first evaluating the DWT based on the Db6 wavelet function. Then, the obtained coefficients are selected by the application of a higher order statistics thresholding. The compressed signal is obtained by linear prediction coding and Huffman coding. The transform domain methods have gained a significant attention due to their capability of accurately represent the ECG signal also at moderate compression ratios. However, most of them are unsuitable for a real-time implementation in acquisition nodes with constrained resources, due to their computational complexity and large buffer memory requirements [11]. Hybrid approaches, combining methods from different categories have been proposed in [11,12]. The method in [11] first detects the beats, it divides each beat into plain and complex blocks, based on their standard deviation. Then, specific compressions are applied to the two block types. The method in [12] faces the problem of unacceptable distortion of abnormal beats for high compression ratios. It uses a Support-Vector Machine (SVM) binary classifier to identify abnormal beats. Then a wavelet-based compression is used for abnormal beats, while normal beats are compressed in groups by means of a hybrid encoder, employing a combination of wavelet and Principal Component Analysis (PCA).

Alternatively, Compressive Sampling (CS) has been proposed for ECG signal compression. The advantage of CS is its capability of achieving performance comparable with transform-domain methods, while moving the computational load from the acquisition node to the receiving node. Since the receiving node is usually located on the Internet cloud, it has much greater computational resources available. Therefore, CS methods allows to realize ECG compression also on sensing nodes with constrained resources. For this reason, CS represents a widely proposed solution for data compression in IoT systems [13], where the acquisition and compression can be implemented in resource-constrained nodes, while the reconstruction is actually carried out (where needed) in the cloud.

The literature regarding the application of CS for ECG compression is mostly concentrated on the quality assessment and improvement of the reconstructed signal by investigating the impact on the quality of a specific *sensing matrix*, *dictionary matrix*, or *reconstruction algorithm*. (see Section 2 for further details about CS) [14]. In [15], the authors compared the performance of the ECG reconstruction with the application of different dictionary matrices, based on the Discrete Wavelet Transform, belonging to several wavelet families, such as Coiflet, Daubechies, Symlet, biorthogonal and reverse biorthogonal. Another comparison of several dictionaries was reported in [14], where the dictionary matrix was based on the Daubechies db4, Gabor, and mexican hat and spline wavelets. Regarding the sensing matrix, often Gaussian and Bernoulli ran-

dom matrices are used as it has been proven their incoherence with Fourier and wavelet dictionaries. In [16], the authors evaluated the Toeplitz, Circulant and Triangular structured sensing matrices, because they do not require the random number generation and therefore are easier to implement and less complex. In [17,18], a CS-based sensing scheme using a Deterministic Binary Block Diagonal matrix (DBBD) as sensing matrix is utilized. In particular, in [17] a hardware implementation of the sensing scheme is also proposed and compared with the random demodulator Analog-to-Information Converter architecture. In [18], a digital CS scheme using the same sensing matrix is proposed and compared with Gaussian random matrices. About reconstruction algorithms, Basis Pursuit (BP) and Orthogonal Matching Pursuit (OMP) are mainly used in the literature. In [16], also Compressed Sampling Matching Pursuit (CoSaMP) and Normalized Iterative Hard Thresholding (NIHT) have been evaluated for ECG reconstruction. Alternative approaches have been proposed in [19] and in [20]. In the former, a parametric model of the ECG signal is used and the signal recovery is achieved by means of the Differential Evolution algorithm. In the latter, a time-normalized agnostic dictionary created by the PCA of training signals is instead used as signal base.

This paper aims to propose a new digital CS-based ECG compression method where a deterministic sensing matrix, adapted to the acquired signal, is utilized. Differently from random sensing matrices, the sensing matrix does not require the random number generation. Moreover, being adapted to the signal, the sensing matrix contains more information on the signal features and therefore it can guarantee a better reconstruction quality, than other deterministic matrices.

The present research aims to realize the ECG signal compression to be integrated in the smart wearable device of the Ambient-intelligent Tele-monitoring and Telemetry for Incepting & Catering over hUman Sustainability (ATTICUS) project [21]. The project main objective is to develop a telemedicine system where physiological signals are acquired by means of a smart T-shirt and possible anomalies in the parameters are discovered.

A preliminary version of the proposed method was presented in [22]. In the work presented here, the aforementioned method was further improved and assessed. In particular, the compression algorithm was modified such that the sensing matrix is not evaluated in each frame, but only whether a significant change in the signal distribution is found. Moreover, the proposed method has been compared against two state of the art methods performing CS-based ECG signal acquisition.

The rest of the paper is organized as follows. In Section 2, some background knowledge about CS is given. In Section 3, the proposed CS-based ECG compression scheme is presented. The experimental evaluation is presented in Section 4. Finally, Section 5 presents the conclusions and future work.

## 2. Fundamentals of compressive sampling

CS is based on the assumption that the ECG signal is sparse in a transform domain, i.e. its representation in such domain is a vector with few elements. In particular, let us consider a vector  $\mathbf{x}$  of  $N$  samples acquired in a certain time window, at Nyquist rate, expressed as:

$$\mathbf{x} = \Psi\theta, \quad (1)$$

where  $\Psi$  is a  $N \times N$  matrix describing the domain transformation, often called *dictionary matrix*, and  $\theta$  is the vector of the coefficients in the transformed domain. The vector  $\theta$  is assumed to be  $K$ -sparse, i.e. it contains at most  $K$  elements. Under the sparsity assumption, the compression is actually performed by multiplying the acquired ECG samples by a  $M \times N$  sensing matrix  $\Phi$ , with  $M < N$ :

$$\mathbf{y} = \Phi \mathbf{x}, \tag{2}$$

where  $\mathbf{y}$  is the  $M$ -size vector of the compressed samples. In order to guarantee the reconstruction, it is necessary that the sensing matrix  $\Phi$  presents a low coherence with the dictionary matrix, where the coherence is defined as [18]:

$$\mu(\Phi, \Psi) = \sqrt{N} \cdot \max_{ij} \frac{\phi_i^T \psi_j}{\|\phi_i\|_2 \|\psi_j\|_2}, \tag{3}$$

where  $\phi_i^T$  and  $\psi_j$  are the  $i$ -th row of  $\Phi$  and the  $j$ -th column of  $\Psi$ , respectively, and  $\|\cdot\|_2$  indicates the  $\ell_2$  norm. The reconstruction of the ECG waveform is actually performed by solving the  $\ell_1$  minimization problem:

$$\hat{\theta} = \arg \min_{\theta} \|\theta\|_1, \text{ subject to: } \mathbf{y} = \Phi \Psi \theta, \tag{4}$$

where  $\|\cdot\|_1$  indicates the  $\ell_1$  norm.

### 3. The proposed method

In this Section, the proposed method is described. In particular, in SubSection 3.1 the compression procedure occurring in the acquisition node is discussed, while in SubSection 3.2 the signal reconstruction, executed at the receiving side, is presented. Furthermore, in Section 3.3 the compressed data rate is described, and in Section 3.4 the computational complexity is analyzed.

#### 3.1. Compression

As mentioned in Section 1, in digital CS-based methods, the compression is operated by multiplying the acquired samples by a sensing matrix. In this paper, the sensing matrix  $\Phi$  is chosen such that the vector  $\mathbf{y}$  performs a sort of cross-correlation between the vector  $\mathbf{x}$ , consisting of a frame of  $N$  samples of the ECG signal acquired at the Nyquist rate, and the pulse train signal  $\mathbf{p}$ , consisting of ones where the signal  $\mathbf{x}$  has a high contribution and zero elsewhere. In this way, the  $M$  samples of  $\mathbf{y}$  contain an information that is somehow related to the auto-correlation coefficients of  $\mathbf{x}$ . The proposed method operates on records of  $N$  samples acquired at Nyquist rate. For each record  $\mathbf{x}$ , the average of the samples in the record is performed to obtain the value  $x_{avg}$ . Then, the signal magnitude  $\mathbf{x}_a$  is evaluated as:

$$\mathbf{x}_a = |\mathbf{X} - x_{avg}|. \tag{5}$$

A threshold value  $x_{th}$  is computed in each frame, representing a certain percentile of the waveform amplitude, by means of a sorting-based algorithm operating on  $x_a$ . Then,  $x_{th}$  is obtained according to the defined percentile. An analysis of the method performance versus the considered percentile is reported in Section 4.2.

The  $\Phi$  matrix is then updated whether a significant change is found in the  $x_{th}$  value. Otherwise, the  $\Phi$  matrix of the previous frame is used. The change of  $x_{th}$  is considered significant when the distance between the value evaluated in the current frame and the one obtained in the previous frame is above a specified limit  $\varepsilon$ .

In the case the  $\Phi$  matrix must be updated, an  $N$ -size binary vector  $\mathbf{p}$  is constructed by quantizing the signal magnitude  $\mathbf{x}_a$ , with the resolution of 1 bit, according to the threshold  $x_{th}$ . Therefore, the  $n$ -th element  $p(n)$  of  $\mathbf{p}$ , with  $n = 0, \dots, N - 1$ , is evaluated as:

$$p(n) = \begin{cases} 1, & \text{if } x_a(n) \geq x_{th} \\ 0, & \text{if } x_a(n) < x_{th} \end{cases}. \tag{6}$$

Once defined the vector  $\mathbf{p}$ , the sensing matrix  $\Phi$  is constructed as follows:

$$\Phi = \begin{bmatrix} p(1) & p(2) & \dots & p(N) \\ p(N - USR + 1) & p(N - USR + 2) & \dots & p(N - USR) \\ \vdots & \vdots & \ddots & \vdots \\ p(USR + 1) & p(USR + 2) & \dots & p(USR) \end{bmatrix} \tag{7}$$

where,  $USR = N/M$  is the *Under-Sampling Ratio*, expressing a measure of the data reduction respect to the number of samples acquired according to the Nyquist criteria. The sensing matrix  $\Phi$  is built as a circulant matrix obtained by shifting the pulse train samples of  $USR$  positions in each row.

The whole compression procedure is summarized by a block scheme as depicted in Fig. 1. For the generic  $n$ -th frame, the  $\mathbf{x}_a$  vector is evaluated as in (5) and the  $x_{th}(n)$  value is obtained, according to the chosen value of percentile. If the current frame is the first one or the absolute difference of  $x_{th}(n)$  and  $x_{th}(n - 1)$  is greater than a certain value  $\varepsilon$ , a new  $\mathbf{p}$  vector is evaluated, applying (6) and a new sensing matrix  $\Phi$  is generated. In this case, it is also necessary to transmit the  $\mathbf{p}$  vector. If instead  $n > 1$  and no significant change occurred in  $x_{th}$  (i.e.  $\|x_{th}(n) - x_{th}(n - 1)\| < \varepsilon$ ), the values of  $\mathbf{p}$  and  $\Phi$  of the previous frame are used. Once defined the sensing matrix to be used, the acquired samples are compressed by the (2) and the compressed samples are transmitted.

#### 3.2. Reconstruction

As mentioned in Section 1, the ECG signal waveform is reconstructed by finding the coefficients in the sparsity domain by solving (4). To this aim, a key role is played by the dictionary matrix (i.e.  $\Psi$ ) which defines the sparsity domain. In other words, the dictionary matrix allows transforming the vector of the acquired samples (see Eq. (1)) to a sparse vector, i.e., having a reduced number of elements.

As reported in [14], the dictionary that achieves the highest reconstruction performance for the ECG signal is obtained by means of the Mexican hat wavelet kernel. In [23], the Mexican hat wavelet matrix  $\Psi_{base}$  is defined as:

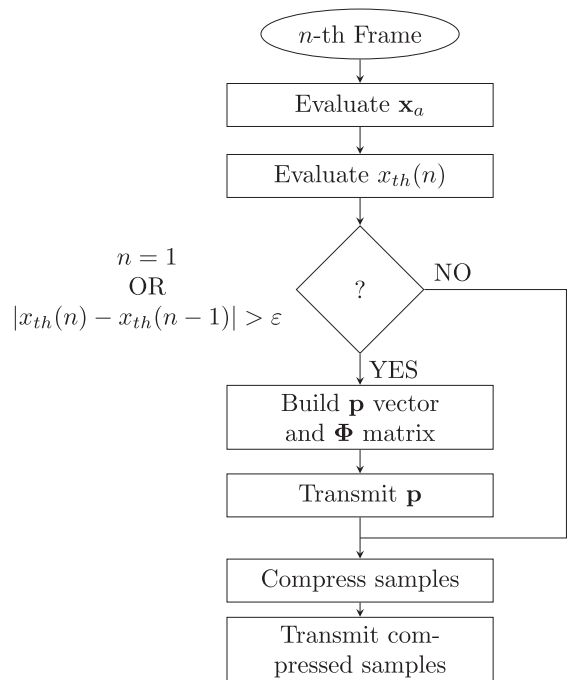


Fig. 1. Block diagram of the compression procedure. The  $\Phi$  matrix is actually evaluated only whether a significant change is found in the value of  $x_{th}$ .

$$\Psi_{base} = \left[ \psi(2, 0), \psi(2, 2), \psi(2, 4), \dots, \psi\left(2, 2\left\lfloor \frac{N-1}{2} \right\rfloor\right), \psi(4, 0), \right. \\ \left. \psi(4, 4), \psi(4, 8), \dots, \psi\left(4, 4\left\lfloor \frac{N-1}{4} \right\rfloor\right), \dots, \psi(N, 0) \right] \quad (8)$$

where  $\psi(a, b)$  is a  $N$ -size vector that describes the Mexican hat wavelet function, defined according to the following expression:

$$\psi(a, b) = \frac{2}{\sqrt{3a} \cdot \pi^{1/4}} \cdot \left[ 1 - \left( \frac{\mathbf{n} - b}{a} \right)^2 \right] \cdot e^{-\frac{1}{2} \left( \frac{\mathbf{n} - b}{a} \right)^2} \quad (9)$$

with  $\mathbf{n} = [0, \dots, N-1]^T$ ,  $a$  the scaling factor,  $a = 2^m$ ,  $m \in \{1, \dots, \lfloor \log_2(N) \rfloor\}$ , and  $b$  the delay factor, which depends on  $a$ , i.e.  $b \in \{0, a, 2a, \dots, a\lfloor \frac{N-1}{a} \rfloor\}$ . Finally, in order to allow the reconstruction of the observed ECG signal in presence of a low-frequency baseline wander, the vector  $\mathbf{u} = [1/N, \dots, 1/N]^T$  is added as last column of the matrix  $\Psi$  that is finally expressed as:

$$\Psi = [\Psi_{base}, \mathbf{u}]. \quad (10)$$

### 3.3. Compressed data rate

Since in the proposed CS method, the sensing matrix is adapted to the signal, it is necessary to provide, for the reconstruction purpose, a coded version of the vector  $\mathbf{p}$  together with the compressed samples, whenever the sensing matrix is updated. By assuming that each sample is provided with a resolution of  $b$  bits, the resulting compression ratio is slightly lower than the undersampling ratio:

$$CR = \frac{B_0}{B_c} = \frac{bNN_f}{bMN_f + N_p N} = \frac{USR}{1 + USR \frac{N_p}{N_f}}, \quad (11)$$

where  $B_0$  and  $B_c$  are the data rates before and after the compression, respectively,  $N_f$  is the number of frames and  $N_p$  is the number of frames where the matrix is updated.

### 3.4. Computational complexity

The proposed CS method presents a very low computational complexity for the acquisition node. For each acquired frame, the following operations are needed:

- $N \log_2 N$  for the evaluation of the percentile  $x_{th}$ , considering that a merge sorting algorithm is used;
- one subtraction and two comparisons to check for a significant change in the  $x_{th}$ ;
- if it is needed to update the  $\Phi$  matrix,  $N$  further comparisons are needed to build the  $\mathbf{p}$  vector;
- $N_1 - 1$  additions, where  $N_1$  is the number of ones in the  $\mathbf{p}$  vector, for each compressed sample are needed to evaluate the compressed frame.

The actual value of  $N_1$  varies in each frame. However, its mean value depends on the considered percentile for the evaluation of the threshold  $x_{th}$ . Indicating with  $p\%$  the value of the percentile:

$$E\{N_1\} = N \cdot P\{x(n) > x_{th}\} = N \left( 1 - \frac{p\%}{100} \right), \quad (12)$$

where  $E\{\cdot\}$  represents the expectation operator, and  $P\{\cdot\}$  is the probability of finding  $x(n)$  samples higher than  $x_{th}$ . Therefore, for each frame, the following mean number of operations is needed in the worst case when the  $\Phi$  matrix is updated:

$$E\{N_{ops}\} = N \log_2 N + N + 3 + M(E\{N_1\} - 1) = \\ = N \left[ M \left( 1 - \frac{p\%}{100} \right) + \log_2 N + 1 \right] - M + 3. \quad (13)$$

Considering, as an example, a record of  $N = 720$  samples acquired at a sampling frequency of 360 Samples/s,  $USR = 4$  and  $p\% = 60$ , according to (13), the number of operations for each record is slightly less than 60000, corresponding to about 30000 operations per second. Such computational load can be easily sustained by a 32-bit microcontroller, based on the ARM Cortex M4F core, which provides at least 1.27 DMIPS (Dhrystone Millions of Instructions Per Second)/MHz and a clock frequency greater than 50 MHz.

At the receiving side, the ECG signal waveform needs to be reconstructed. At this stage, the computational complexity depends on the chosen reconstruction algorithm. BP has generally a complexity  $\mathcal{O}(N^3)$ . OMP has instead a much lower computational load. In its implementation based on the matrix inversion lemma, the number of operations is [24]:

$$N_{ops} = \mathcal{O}((N + M)S), \quad (14)$$

where,  $S$  is the number of iterations of the OMP algorithm which is in any case lower than  $N$ .

## 4. Results and discussion

In this Section, the performance of the method presented in Section 3 is analyzed through several tests implemented in MATLAB. For testing purposes, the ECG signals from the PhysioNet MIT-BIH Arrhythmia Database (available online [25]) have been considered. The MIT BIH database was chosen among the Internet-available ones as it is the most widely used in the scientific literature. Therefore, the results obtained on the ECG signals of this database can be easily compared among several research papers. This database contains 48 half-hour excerpts of two-channel ambulatory ECG recordings, obtained from 47 subjects studied by the BIH Arrhythmia Laboratory. The recordings were acquired at a 360 Hz sampling frequency per channel with 11-bit resolution over a 10 mV range. The signals were segmented in  $N = 720$ -size frames, while  $M$  depends on the adopted  $USR$  value. Before being processed by the proposed CS method, in each frame the first three harmonics of the power-line signal, at {60; 120; 180} Hz, respectively have been removed in the frequency domain [26].

Preliminary assessment phases were conducted on the method with the following aims: (i) to evaluate the method with different reconstruction algorithms, (ii) to tune the amplitude percentile used in the method to build the  $\mathbf{p}$  vector, (iii) to verify the influence of the  $\varepsilon$  threshold, which controls the update of the sensing matrix. In the above mentioned phases, two data-sets of ten ECG signals from [25] have been used:

$$S_1 = \{100, 106, 107, 115, 117, 118, 119, 221, 223, 228\} \quad (15)$$

$$S_2 = \{101, 109, 122, 124, 200, 202, 205, 217, 219, 234\} \quad (16)$$

The first data-set contains the following main beat labels: atrial premature beats, premature ventricular contractions, paced beats, isolated QRS-like artifacts, and right bundle branch block beats. In the second data-set, the main beat labels are: left bundle branch block beats, aberrated atrial premature beats, non-conducted P-waves, and nodal (junctional) premature beats. For each ECG signal, the Percentage of Root-mean-squared Difference (PRD) has been evaluated as figure of merit [14,27–29]. The PRD is computed as follows:

$$PRD = \frac{\|\mathbf{x} - \hat{\mathbf{x}}\|_2}{\|\mathbf{x}\|_2} \times 100\%, \quad (17)$$

where  $\mathbf{x}$  and  $\hat{\mathbf{x}}$  are the original and the reconstructed signal, respectively. Then, two evaluation phases have been carried out. In the former, the method is characterized on the above mentioned signal data-sets and compared with the method proposed in [18] (DBBD

sensing matrix and DCT dictionary) and the method reporting the best result in [14] (Bernoulli sensing matrix and two scales Mexican hat based dictionary). Those methods were selected as they got the better accuracy of reconstruction within CS-based methods. In this analysis the following figures of merit were evaluated: PRD, PRD Normalized (PRDN), Mean Square Error (MSE), Root Mean Square Error (RMSE), Peak Signal to Noise Ratio (PSNR). The used expression of PRD is that reported in (17). The following expressions of PRDN, MSE, RMSE and PSNR have been used [12]:

$$PRDN = \frac{\|\mathbf{x} - \hat{\mathbf{x}}\|_2}{\|\mathbf{x} - \bar{\mathbf{x}}\|_2} \times 100\%, \quad (18)$$

$$MSE = \frac{\|\mathbf{x} - \hat{\mathbf{x}}\|_2}{N_s}, \quad (19)$$

$$RMSE = \sqrt{\frac{\|\mathbf{x} - \hat{\mathbf{x}}\|_2}{N_s}}, \quad (20)$$

$$PSNR = 10 \log_{10} \frac{\max(\mathbf{x})^2}{MSE}, \quad (21)$$

where  $\bar{\mathbf{x}}$  is the average of the elements of  $\mathbf{x}$ , and  $N_s$  is the number of samples of the entire signal under observation.

In the latter phase, the method was tested on several types of abnormal beats, by evaluating the Weighted Diagnostic Distortion (WDD) [30], and the Wavelet Energy-based Diagnostic Distortion (WEDD) [31]. WEDD was evaluated according to [31] as a weighted sum of the Wavelet PRD (WPRD):

$$WEDD = \sum_{l=1}^{L+1} w_l WPRD_l \quad (22)$$

where  $L$  is the number of wavelet levels. The weights  $w_l$  and the WPRD are evaluated as:

$$w_l = \frac{\sum_{k=1}^{K_l} d_l^2(k)}{\sum_{m=1}^L L + 1 \sum_{k=1}^{K_m} K_m d_m^2(k)} \quad (23)$$

$$WPRD_l = \sqrt{\frac{\sum_{k=1}^{K_l} [d_l(k) - \tilde{d}_l(k)]^2}{\sum_{k=1}^{K_l} d_l^2(k)}} \quad (24)$$

where,  $K_l$  denotes the number of wavelet coefficients at the  $l$ -th level,  $d_l(k)$  and  $\tilde{d}_l(k)$  are the  $k$ -th wavelet coefficients of the original and of the reconstructed signal, respectively.

WDD was evaluated according to [12], by considering the following features: (i) QRS duration, (ii) P-wave height, (iii) P-wave duration, (iv) R-R interval, (v) QRS amplitude, (vi) PR interval, (vii) QT interval, and (viii) T-wave height. The features were evaluated by applying the method proposed in [32] for ECG delineation. For the evaluation of WDD, the following matrix of weights was used [12]:

$$\Lambda = \text{diag}([22221111]). \quad (25)$$

Therefore, WDD is evaluated as:

$$WDD = \Delta\beta^T \cdot \frac{\Lambda}{\text{tr}(\Lambda)} \cdot \Delta\beta \times 100, \quad (26)$$

where,  $\Delta\beta$  is the vector of the normalized differences  $\Delta\beta_i$  of the features evaluated on the original and reconstructed signal, respectively [30]:

$$\Delta\beta_i = \frac{|\beta_i - \hat{\beta}_i|}{\max\{\beta_i, \hat{\beta}_i\}}. \quad (27)$$

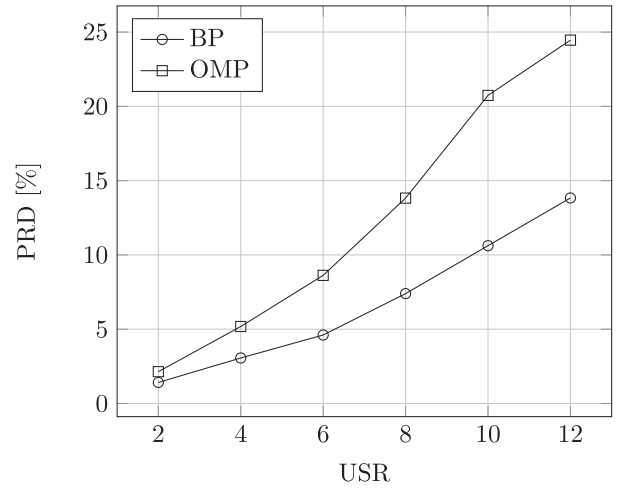


Fig. 2. Average PRD over the  $S_1$  data-set using BP and OMP as reconstruction algorithms. BP achieves a better reconstruction quality for all the considered values of USR.

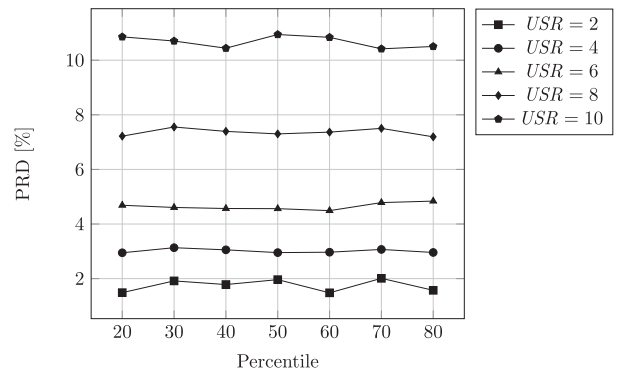


Fig. 3. Average PRD of the proposed method versus the percentile and for several values of the USR.

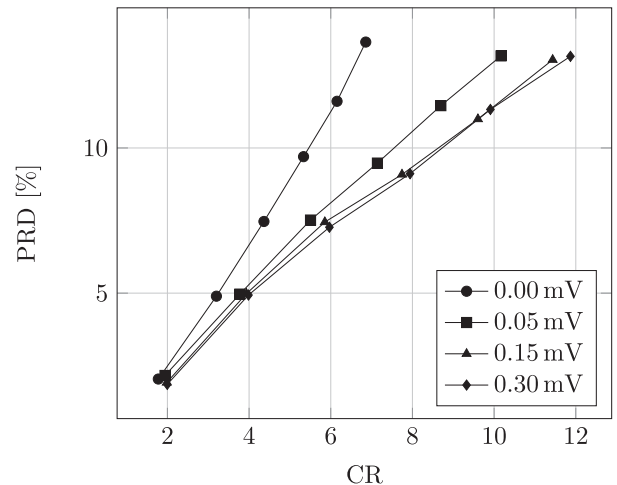


Fig. 4. Average PRD, evaluated on the first 5 min of the signals in the  $S_1$  data-set, for different values of USR and three values of the threshold  $\epsilon$ : 0.00 mV (sensing matrix changes in all the frames), 0.05 mV, 0.15 mV, and 0.30 mV.

#### 4.1. Influence of the reconstruction algorithm

In this test, the performance of the proposed method, by employing either the OMP or BP algorithms in the signal reconstruction, has been evaluated in terms of *PRD* averaged among all the signals of the  $S_1$  data-set. The analysis has been carried out on the first 5 min of the signal recordings, considering values of the *USR* ranging from 2 up to 12 with a step of 2. The obtained results are shown in Fig. 2. As it was expected, the proposed method exhibits lower *PRD* if the BP algorithm is employed instead of OMP. In particular, by considering a *PRD* less than 9%, which represents a good signal reconstruction quality for medical applications [28], the OMP algorithm can be adopted with a maximum *USR* of 6, while the BP algorithm allows to increase the *USR* at a maximum value of 9. However, the BP algorithm exhibits a computational complexity higher than the OMP. Since it assures a better

accuracy in terms of signal quality reconstruction, BP was used in this paper.

#### 4.2. Influence of percentile

This analysis aims at evaluating the influence of the percentile used for the determination of the threshold  $x_{th}$ . To this aim, the average *PRD* over the first 1min of the signals contained in the  $S_1$  data-set was evaluated for different percentiles and *USR* values. Each signal is reconstructed through the BP algorithm. The analysis has been carried out according to percentile values ranging from 20% to 80%, with a step of 10% and for *USR* values equal to {2, 4, 6, 8, 10}. In Fig. 3, the obtained results are depicted. From this figure, it can be noted that the *PRD* does not show significant changes with the percentile in the considered range, for all the *USR* values. A value of 60% has been chosen for the further tests.

**Table 1**

Comparison of the results obtained with the proposed method (Proposed) vs. the method proposed in [18] (DBBD + DCT) and the method reporting the best results in [14] (Bernoulli + MexHat2) for the Data-set  $S_1$ : (a) average, (b) standard deviation.

<i>USR</i>	Method	<i>CR</i>	<i>PRD</i> [%]	<i>PRDN</i> [%]	<i>MSE</i> [ $\cdot 10^{-5}$ mV <sup>2</sup> ]	<i>RMSE</i> [ $\cdot 10^{-3}$ mV]	<i>SNR</i> [dB]	<i>PSNR</i> [dB]
2	Proposed	2.00	1.42	2.30	2.39	4.87	37.72	50.41
	DBBD+DCT	2.00	0.94	1.52	1.58	3.97	41.22	52.16
	Bernoulli+MexHat2	2.00	2.75	4.29	4.75	6.85	31.86	47.47
4	Proposed	3.99	3.06	4.68	5.04	7.04	31.39	47.24
	DBBD+DCT	4.00	3.35	5.00	5.47	7.23	31.21	47.15
	Bernoulli+MexHat2	4.00	4.91	7.49	8.32	9.04	27.09	45.09
6	Proposed	5.97	4.61	7.24	8.16	8.93	27.34	45.22
	DBBD+DCT	6.00	8.21	13.38	14.36	11.79	22.60	42.85
	Bernoulli+MexHat2	6.00	7.59	11.80	13.31	11.40	23.10	43.10
8	Proposed	7.94	7.40	11.71	13.04	11.31	23.18	43.14
	DBBD+DCT	8.00	14.46	23.72	25.10	15.57	17.78	40.43
	Bernoulli+MexHat2	8.00	11.41	17.88	20.05	14.01	19.49	41.29
10	Proposed	9.91	10.62	17.21	18.99	13.66	19.91	41.50
	DBBD+DCT	10.00	19.48	31.88	33.56	18.05	15.18	39.13
	Bernoulli+MexHat2	10.00	16.97	27.14	29.65	17.05	16.07	39.58

(a) Data-set  $S_1$  average.

<i>USR</i>	Method	<i>CR</i>	<i>PRD</i> [%]	<i>PRDN</i> [%]	<i>MSE</i> [ $\cdot 10^{-5}$ mV <sup>2</sup> ]	<i>RMSE</i> [ $\cdot 10^{-3}$ mV]	<i>SNR</i> [dB]	<i>PSNR</i> [dB]
2	Proposed	2.00	0.60	1.00	0.39	0.40	3.86	6.23
	DBBD+DCT	2.00	0.39	0.57	0.17	0.21	3.53	6.29
	Bernoulli+MexHat2	2.00	1.12	1.04	1.19	0.84	3.57	5.88
4	Proposed	3.99	1.64	1.66	1.28	0.91	4.63	5.81
	DBBD+DCT	4.00	2.15	2.75	2.58	1.65	5.89	5.27
	Bernoulli+MexHat2	4.00	2.36	2.05	2.41	1.30	4.22	5.71
6	Proposed	5.97	1.80	1.84	2.72	1.45	3.51	5.86
	DBBD+DCT	6.00	3.63	6.89	5.49	2.27	4.34	5.71
	Bernoulli+MexHat2	6.00	3.15	3.06	4.60	1.90	3.76	5.79
8	Proposed	7.94	2.73	3.07	3.96	1.64	3.35	5.97
	DBBD+DCT	8.00	7.21	12.44	9.88	3.06	4.37	5.98
	Bernoulli+MexHat2	8.00	4.38	4.75	6.16	2.15	3.64	5.60
10	Proposed	9.91	3.35	5.07	5.66	1.95	2.98	6.11
	DBBD+DCT	10.00	9.73	15.84	12.12	3.30	4.32	6.08
	Bernoulli+MexHat2	10.00	6.39	10.36	8.59	2.52	3.78	5.58

(b) Data-set  $S_1$  standard deviation.

4.3. Influence of the  $\varepsilon$  threshold

In Fig. 4, the results in terms of average PRD, evaluated on the first 5 min of the signals in the  $S_1$  data-set when different values of the  $USR$  and  $\varepsilon$  have been used, are shown. The PRD is reported versus the CR, which, as mentioned above, is slightly lower than the  $USR$ , due to the need of transmitting the  $\mathbf{p}$  vector, whenever it is updated. In details, the number of times when  $\mathbf{p}$  is updated is controlled by the value  $\varepsilon$ . Higher  $\varepsilon$  is, lower is the probability that  $\mathbf{p}$  is updated and CR is closer to  $USR$ . It can be observed in Fig. 4 that the PRD does not change significantly by increasing  $\varepsilon$  up to 0.30 mV, while a relevant increase of CR is achieved. For this reason a value of  $\varepsilon$  of 0.30 mV is selected for the further tests.

4.4. Experimental results

The results of the former evaluation phase are shown in Table 1 and Table 2, where the values of the considered figures of merit are reported versus the  $USR$  in the case of the proposed method (Proposed), of the method proposed in [18] (DBBD + DCT) and the method reporting the best results in [14] (Bernoulli + MexHat2). In particular, Table 1 reports the results for Data-set  $S_1$ , while Table 2 reports the results for Data-set  $S_2$ . In each table, the average and standard deviations of each figure of merit over the signals included in the Data-set are given.

The  $USR$  is therefore reported in the first column. The second column reports the method and the third column shows the

**Table 2**  
Comparison of the results obtained with the proposed method (Proposed) vs. the method proposed in [18] (DBBD + DCT) and the method reporting the best results in [14] (Bernoulli + MexHat2) for the Data-set  $S_2$ : (a) average, (b) standard deviation.

$USR$	Method	$CR$	$PRD$ [%]	$PRDN$ [%]	$MSE$ [ $\cdot 10^{-5} \text{ mV}^2$ ]	$RMSE$ [ $\cdot 10^{-3} \text{ mV}$ ]	$SNR$ [dB]	$PSNR$ [dB]
2	Proposed	2.00	1.83	2.47	2.66	5.06	36.10	51.24
	DBBD+DCT	2.00	0.97	1.38	1.45	3.80	40.86	53.62
	Bernoulli+MexHat2	2.00	2.93	4.10	4.46	6.65	31.18	48.78
4	Proposed	3.98	3.33	4.63	4.91	6.96	30.44	48.41
	DBBD+DCT	4.00	3.29	4.47	4.93	6.85	31.02	48.70
	Bernoulli+MexHat2	4.00	5.48	7.58	8.17	8.98	25.99	46.19
6	Proposed	5.96	4.98	7.02	7.53	8.60	26.77	46.58
	DBBD+DCT	6.00	7.41	10.72	11.11	10.39	23.60	44.99
	Bernoulli+MexHat2	6.00	8.21	11.48	12.47	11.08	22.35	44.37
8	Proposed	7.92	7.79	10.94	11.60	10.72	22.89	44.64
	DBBD+DCT	8.00	12.57	18.26	18.46	13.34	19.34	42.86
	Bernoulli+MexHat2	8.00	11.75	16.70	18.04	13.33	19.15	42.77
10	Proposed	9.88	10.63	15.06	16.12	12.64	19.99	43.19
	DBBD+DCT	10.00	17.50	25.57	25.98	15.81	16.44	41.41
	Bernoulli+MexHat2	10.00	16.68	24.14	25.49	15.82	16.22	41.30

(a) Data-set  $S_2$  average.

$USR$	Method	$CR$	$PRD$ [%]	$PRDN$ [%]	$MSE$ [ $\cdot 10^{-5} \text{ mV}^2$ ]	$RMSE$ [ $\cdot 10^{-3} \text{ mV}$ ]	$SNR$ [dB]	$PSNR$ [dB]
2	Proposed	2.00	1.22	1.11	1.24	1.03	4.92	2.40
	DBBD+DCT	2.00	0.36	0.40	0.18	0.24	3.41	2.51
	Bernoulli+MexHat2	2.00	1.04	0.80	0.93	0.70	3.29	2.28
4	Proposed	3.98	1.57	1.52	1.31	0.91	4.23	2.40
	DBBD+DCT	4.00	1.80	1.77	2.33	1.63	5.37	2.70
	Bernoulli+MexHat2	4.00	2.31	1.95	2.00	1.11	3.95	2.27
6	Proposed	5.96	2.15	2.19	2.13	1.20	3.79	2.48
	DBBD+DCT	6.00	3.50	5.48	3.74	1.86	4.54	2.82
	Bernoulli+MexHat2	6.00	3.31	2.83	3.34	1.47	3.57	2.27
8	Proposed	7.92	2.98	3.13	2.42	1.14	3.98	2.54
	DBBD+DCT	8.00	6.84	10.75	6.81	2.70	5.26	2.92
	Bernoulli+MexHat2	8.00	4.21	4.79	4.65	1.77	3.39	2.46
10	Proposed	9.88	3.69	3.70	3.02	1.20	3.27	2.38
	DBBD+DCT	10.00	9.40	14.04	9.92	3.33	5.25	3.07
	Bernoulli+MexHat2	10.00	6.63	9.68	6.65	2.29	3.64	2.65

(b) Data-set  $S_2$  standard deviation.

obtained CR. It can be seen that the proposed method shows average values of the figures of merit that are better than the method Bernoulli + MexHat2 for all the considered values of CR. Compared with the method [18], the proposed method shows results that are slightly worse for  $USR = 2$ . Both the methods then give similar values for  $USR = 4$ . For  $USR > 4$  the proposed method shows a much better accuracy. Looking at the standard deviations, it can be observed that, for both Data-sets  $S_1$  and  $S_2$ , the proposed method shows a lower variability, for almost all the figures of merit, for a CR higher than 2.

The superiority of the proposed method can be better observed in Fig. 5, where the trend of the average PRD (solid line) and the maximum PRD (dashed line), evaluated on the signals belonging to the Data-sets  $S_1$  (Fig. 5a) and  $S_2$  (Fig. 5b), respectively, are reported versus the CR for the three methods. It can be seen that for  $CR > 4$  the proposed method achieves a huge average reduction of PRD compared with both the other methods on both the data-sets. Moreover, it shows also a lower variability than the other methods. The higher accuracy of the proposed method than the other methods is due to the adaptation of the sensing matrix to the acquired signal, realized by evaluating and transmitting the  $\mathbf{p}$  vector.

The latter evaluation phase was devoted to verify the behavior of the proposed method in the case of abnormal beats. To this aim, abnormal beats of 4 types were selected in the first 10min of the signal recordings No. 222 (atrial premature beat - A), No. 105

(premature ventricular contraction - V), No. 213 (fusion of ventricular and normal beat - F), and No. 111 (left bundle branch block beat - L).

The results are reported in Table 3. The table reports in the first column the type of abnormal beat and the number of analyzed beats. In the second column, the  $USR$  is reported. The other columns report the average values and the standard deviation of the  $WDD$  and  $WEDD$  figures of merit, respectively, evaluated on the considered beats. As expected, the values of both  $WDD$  and  $WEDD$  increase with the  $USR$ . However, for all the considered types of beats and values of  $USR$ , the values of  $WDD$  and  $WEDD$  result in the ranges of the highest quality categories reported in [30,31]. Slightly higher values were found for A and V beat types, mainly for  $USR = 8$ . This can be due to a non-perfect coverage of the used Mexican hat dictionary for specific beat types. This will be analyzed in a further work where an automatic optimization of the dictionary is planned, with the application of the method proposed in [33].

The good reconstruction quality of abnormal beats can be seen in Fig. 6, where the acquired waveforms (thick grey line) and the reconstructed ones (thin black line), corresponding to 4 frames centered around abnormal beats of different types, after the signal has been compressed with  $USR = 8$ . In particular, atrial premature beat, premature ventricular contraction, fusion of ventricular and normal beat and left bundle branch block beat are reported in Fig. 6a–d, respectively. It can be seen a good overposition of the

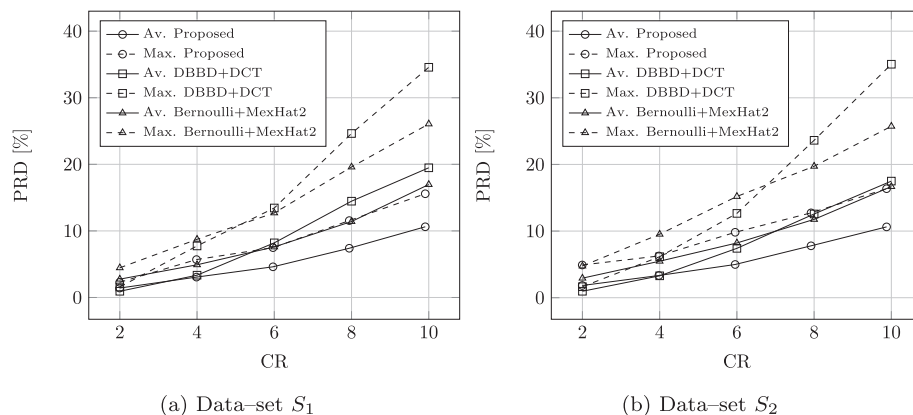
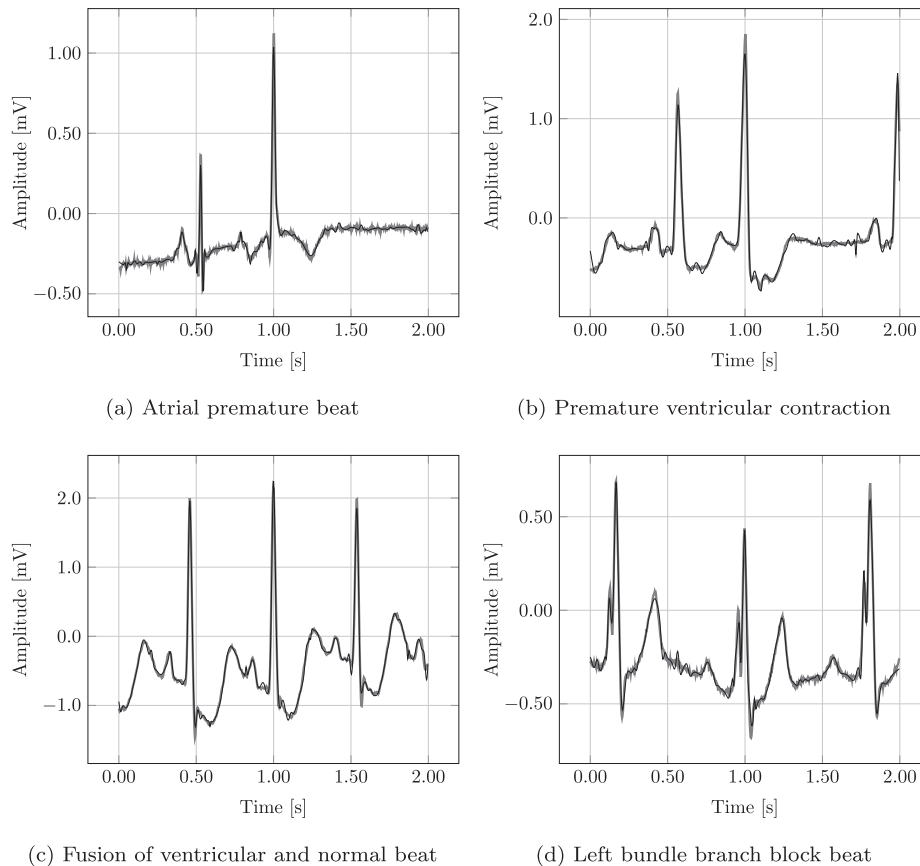


Fig. 5. Average PRD (solid line) and Maximum PRD (dashed line) obtained for the  $S_1$  (a) and  $S_2$  (b) for the proposed method (Proposed), the method proposed in [18] (DBBD + DCT), and the method reporting the best performance of [14] (Bernoulli + MexHat2).

Table 3  
Results of  $WDD$  and  $WEDD$  for 4 types of abnormal beats for different values of the  $USR$ .

Abnormal beat type	$USR$	$WDD$ [%]		$WEDD$ [%]	
		Average	Standard deviation	Average	Standard deviation
A (100 beats)	2	0.7	2.1	4.1	3.7
	4	0.9	1.6	5.0	2.2
	6	1.9	3.4	8.2	3.6
	8	3.3	4.1	13.3	7.0
V (41 beats)	2	2.08	4.05	0.96	0.52
	4	3.91	5.22	4.75	3.33
	6	3.16	3.97	7.36	4.35
	8	3.78	5.02	12.72	7.37
F (100 beats)	2	0.09	0.25	0.42	0.23
	4	0.28	0.37	1.79	0.81
	6	0.85	1.15	4.44	1.94
	8	1.82	2.78	8.94	3.67
L (100 beats)	2	0.20	0.60	1.94	1.30
	4	0.20	0.67	2.67	1.27
	6	0.42	0.93	5.63	2.70
	8	1.06	1.22	10.54	4.79



**Fig. 6.** Original waveforms (dashed grey line) and reconstructed waveform (solid black line) of some abnormal beats extracted from the MIT-BIH arrhythmia database signals, after a compression with  $USR = 8$ : (a) atrial premature beat (Signal No. 222), (b) premature ventricular contraction (Signal No. 105), (c) left bundle branch block (Signal No. 213), and (d) fusion of ventricular and normal beat (Signal No. 111).

thin black line (reconstructed signal) over the thick grey line (original acquired signal) that allows preserving all the characteristic features of the waveform.

## 5. Conclusion

In this paper, a novel method for the compressive sampling of ECG signals, is presented. The method is based on the idea of building a sensing matrix, which is adapted on the acquired signal frame. In particular, it is a circulant matrix, containing zeros and ones, obtained by quantizing (with the resolution of 1 bit) the magnitude of the acquired signal. The adapted sensing matrix guarantees that the significant portions of the signal waveform are actually contained in the compressed version, thus allowing a more accurate reconstruction respect to the methods already available in scientific literature. The sensing matrix is then used in combination with a modified Mexican hat wavelet dictionary that allows also the reconstruction of the signal wander for each processed frame.

The experimental results, obtained on signal recordings from the PhysioNet MIT-BIH Arrhythmia Database, showed that the proposed method achieves a better accuracy in ECG signal reconstruction than the other methods based on compressive sampling. The good ECG signal reconstruction accuracy was also confirmed on abnormal beats of several types.

Future work will be focused on a further improvement of the used dictionary, such to better adapt it to the different ECG signal waveforms. Moreover, the implementation and testing of the proposed method on an IoMT system is planned.

## Declaration of Competing Interest

The authors declare that they have no known competing financial interests or personal relationships that could have appeared to influence the work reported in this paper.

## Acknowledgment

The paper has been supported by the PON project ARS01\_00860 “Ambient-intelligent Tele-monitoring and Telemetry for Incepting & Catering over hUman Sustainability (ATTICUS)”, RNA/COR 576347. The authors would like to thank Prof. Pasquale Daponte for his helpful suggestions during all the phases of the research.

## References

- [1] D. Dias, J.P.S. Cunha, Wearable health devices-vital sign monitoring, systems and technologies, *Sensors*, MDPI (Basel) 18 (8) (2018) 2414.
- [2] S. Shirmohammadi, K. Barbé, D. Grimaldi, S. Rapuano, S. Grassini, Instrumentation and measurement in medical, biomedical, and healthcare systems, *IEEE Instr. & Meas. Magaz.* 19 (5) (2016) 6–12.
- [3] E. Balestrieri, P. Daponte, L. De Vito, F. Picariello, S. Rapuano, I. Tudosa, A Wi-Fi IoT prototype for ECG monitoring exploiting a novel Compressed Sensing method, *Acta IMEKO* (2).
- [4] M. Tlili, M. Ben-Romdhane, A. Maalej, F. Rivet, D. Dallet, C. Rebai, Level-crossing ADC design and evaluation methodology for normal and pathological electrocardiogram signals measurement, *Measurement* 124 (February) (2018) 413–425, ISSN 02632241.
- [5] C.K. Jha, M.H. Kolekar, Electrocardiogram data compression using DCT based discrete orthogonal Stockwell transform, *Biomed. Signal Process. Control* 46 (2018) 174–181, ISSN 17468108.

- [6] S. Mukhopadhyay, S. Mitra, M. Mitra, An ECG signal compression technique using ASCII character encoding, *Measurement* 45 (6) (2012) 1651–1660, ISSN 02632241.
- [7] K. Luo, J. Li, J. Wu, A dynamic compression scheme for energy-efficient real-time wireless electrocardiogram biosensors, *IEEE Trans. Instrum. Meas.* 63 (9) (2014) 2160–2169, ISSN 00189456.
- [8] Y. Zigel, A. Cohen, A. Katz, ECG signal compression using analysis by synthesis coding, *IEEE Trans. Biomed. Eng.* 47 (10) (2000a) 1308–1316, ISSN 00189294.
- [9] N. Adochiei, V. David, F. Adochiei, I. Tudosa, ECG waves and features extraction using wavelet multi-resolution analysis, in: *Proc. of E-Health and Bioengineering Conference (EHB)*, Iasi, 1–4, 2011.
- [10] S.A. Chouakri, O. Djaafri, A. Taleb-Ahmed, Wavelet transform and Huffman coding based electrocardiogram compression algorithm: application to telecardiology, *J. Phys.: Conf. Ser.* 454 (1), ISSN 17426596.
- [11] P. Bera, R. Gupta, Hybrid encoding algorithm for real time compressed electrocardiogram acquisition, *Measurement* 91 (2016) 651–660, ISSN 02632241.
- [12] P. Bera, R. Gupta, J. Saha, Preserving abnormal beat morphology in long-term ECG recording: an efficient hybrid compression approach, *IEEE Trans. Instrum. Meas.* 69 (5) (2020) 2084–2092, ISSN 0018–9456.
- [13] E. Balestrieri, L. De Vito, F. Lamonaca, F. Picariello, S. Rapuano, I. Tudosa, Research challenges in measurement for Internet of Things systems, *ACTA IMEKO* 7 (4) (2018) 82–94.
- [14] D. Craven, B. McGinley, L. Kilmartin, M. Glavin, E. Jones, Compressed sensing for bioelectric signals: a review, *IEEE J. Biomed. Health Inform.* 19 (2) (2015) 529–540.
- [15] A. Mishra, F. Thakkar, C. Modi, R. Kher, Comparative analysis of wavelet basis functions for ECG signal compression through compressive sensing, *Int. J. Comput. Sci. Telecommun.* 3 (5) (2012) 23–31.
- [16] A.M.R. Dixon, E.G. Allstot, D. Gangopadhyay, D.J. Allstot, Compressed sensing system considerations for ECG and EMG wireless biosensors, *IEEE Trans. Biomed. Circ. Syst.* 6 (2) (2012) 156–166.
- [17] A. Ravelomanantsoa, S. Member, H. Rabah, S. Member, Simple and efficient compressed sensing encoder for wireless body area network, *IEEE Trans. Instrum. Meas.* 63 (12) (2014) 2973–2982.
- [18] A. Ravelomanantsoa, H. Rabah, A. Rouane, Compressed sensing: a simple deterministic measurement matrix and a fast recovery algorithm, *IEEE Trans. Instrum. Meas.* 64 (12) (2015) 3405–3413, ISSN 00189456.
- [19] L. Michaeli, J. Šaliga, P. Dolinský, I. Andráš, Optimization paradigm in the signal recovery after compressive sensing, *Meas. Sci. Rev.* 19 (1) (2019) 35–42, ISSN 13358871.
- [20] P. Dolinský, I. Andráš, J. Šaliga, L. Michaeli, Reconstruction for ECG compressed sensing using a time-normalized PCA dictionary, in: *Proc. of the 12th Int. Conf. on Measurement*, MEASUREMENT 2019, 30–33, ISBN 9788097262938, 2019.
- [21] E. Balestrieri, F. Boldi, A.R. Colavita, L. De Vito, G. Laudato, R. Oliveto, F. Picariello, S. Rivaldi, S. Scalabrino, P. Torchitti, I. Tudosa, The architecture of an innovative smart T-shirt based on the Internet of Medical Things paradigm, in: *Proc. of 2019 IEEE Int. Symp. on Medical Measurements and Applications*, Istanbul, Turkey, 2019.
- [22] E. Balestrieri, L. De Vito, F. Picariello, I. Tudosa, A novel method for compressed sensing based sampling of ECG signals in medical-IoT era, in: *Proc. of 2019 IEEE Int. Symp. on Medical Measurements and Applications*, Istanbul, Turkey, 2019.
- [23] M. Burke, M. Nasor, ECG Analysis using the Mexican-Hat Wavelet, in: *Advances in scientific computing, computational intelligence and applications*, Athens, Greece, 2001, pp. 26–31.
- [24] B.L. Sturm, M.G. Christensen, Comparison of orthogonal matching pursuit implementations, in: *Proc. of 20th European Signal Processing Conference*, Bucharest, Romania, 220–224, 2012.
- [25] MIT-BIH Arrhythmia Database, URL <https://www.physionet.org/physiobank/database/mitdb/>, 2005.
- [26] I. Tudosa, N. Adochiei, LMS algorithm derivatives used in real-time filtering of ECG signals: A study case on performance evaluation, in: *Proc. of Intern. Conf. and Exposition on Electrical and Power Engineering*, 565–570, 2012.
- [27] H. Mamaghanian, N. Khaled, D. Atienza, P. Vandergheynst, Design and exploration of low-power analog to information conversion based on compressed sensing, *IEEE J. Emerg. Select. Top. Circ. Syst.* 2 (3) (2012) 493–501.
- [28] H. Djelouat, X. Zhai, M.A. Disi, A. Amira, F. Bensaali, System-on-Chip solution for patients biometric: a compressive sensing-based approach, *IEEE Sens. J.* 18 (23) (2018) 9629–9639.
- [29] D. Mitra, H. Zanddizari, S. Rajan, Investigation of Kronecker-based recovery of compressed ECG signal, *IEEE Trans. on Instr. and Meas.* 69 (6) (2020) 3642–3653.
- [30] Y. Zigel, A. Cohen, A. Katz, The weighted diagnostic distortion (WDD) measure for ECG signal compression, *IEEE Transactions on Biomedical Engineering* 47 (11) (2000b) 1422–1430, ISSN 00189294.
- [31] M.S. Manikandan, S. Dandapat, Wavelet energy based diagnostic distortion measure for ECG, *Biomed. Signal Process. Control* 2 (2) (2007) 80–96, ISSN 17468094.
- [32] J.P. Martínez, R. Almeida, S. Olmos, A.P. Rocha, P. Laguna, A wavelet-based ECG delineator evaluation on standard databases, *IEEE Trans. Biomed. Eng.* 51 (4) (2004) 570–581, ISSN 00189294.
- [33] E. Picariello, E. Balestrieri, F. Picariello, S. Rapuano, I. Tudosa, L. De Vito, A new method for dictionary matrix optimization in ECG compressed sensing, in: *Proc. of 2020 Int. Symp. on Medical Measurements and Applications*, Bari, Italy, 2020.